Supporting Information

Hye-Ryong Shim et al. 10.1073/pnas.1000806107

SI Text

SI Materials and Methods. ***Cell culture, cloning, and virus generation.*** Sf9 insect cells were maintained in suspension in HyQ-SFX media (HyClone) supplemented with 8% (v/v) heat-inactivated FBS. Hi5 insect cells were maintained in HyQ-SFX without serum. N-acetylglucosaminyltransferase I (GnTI)-deficient Human Embryonic Kindey-293 (HEK293 GnTI$^-$) cells (1) were maintained in CDM4HEK293 media (HyClone) supplemented with 4% heat-inactivated FBS. For pro-PDGF-A, the cDNA fragment encoding residues 1–183 plus a C-terminal 6-His-tag was subcloned into the pVL1393 vector (Invitrogen). For the PDGF-B/PDGFRβ complex, the cDNA fragments encoding the ectodomains of human PDGFRβ (residue 1–314) and human PDGF-B (residue 1–185), attached to a C-terminal seven-histidine tag, were subcloned into the baculovirus mediated mammalian cell gene transduction (BacMam) vector pVLAD6 (2). The constructs and the BacVector-3000 baculovirus DNA (EMD Chemicals) were used to cotransfect sf9 cells in six-well plates in the presence of the InsectGeneJuice transfection reagent (EMD Chemicals). After incubation of the transfected cells at 27 °C for 5 days, the resulting low titer virus stock was harvested, and was used to infect Sf9 cells at 2×10^6 cell/mL for amplification.

Protein expression and purification. For propeptide-bound PDGF-A, three liters of hi5 cells were grown to a density $1.8 \times$ 106 cells/mL and infected with amplified virus at an Multiplicity of Infection (MOI) of 10. After 66 h, the recombinant proteins in the supernatant were captured by the Talon® metal affinity resin (Clontech) and eluted with 300 mM imidazole pH7.5. To obtain fully cleaved PDGF-A/propeptide complex, the above supernatant was incubated at room temperature for 3 d before the his-tagged proteins were captured by the Talon resin. For the PDGF-B/PDGFRβ complex, the amplified PDGF-B and PDGFRβ BacMam viruses were used to infect 1–6 liters of HEK293 GnTI$^-$ cells individually at a density of $1.0–1.5 \times 10^6$ cells/mL. After 72 h, the cells were pelleted, and the supernatants were mixed at appropriate ratio. The complex were captured by the Talon affinity resin and eluted with 300 mM imidazole pH 7.5. The eluted PDGF-B/PDGFRβ complex was glycan-minimized using Endoglycosidase-F1 (SIGMA) and treated with bovine carboxypeptidase-A (SIGMA) for his-tag removal. All the proteins were further purified with size exclusion columns (Superdex-200, Amersham Biosciences) preequilibrated and eluted with Hepes-buffered saline (HBS) buffer (10 mM Hepes pH7.5, 150 mM NaCl), and concentrated to 10 mg/mL.

Crystallization.
Crystallization was performed using the sitting-drop vapor diffusion method at 22 °C, with the drops containing equal volumes of protein solution and reservoir solution equilibrated against the reservoir solution. For the PDGF-A/propeptide complex, the reservoir solution is 1.0 M sodium citrate, 0.1 M imidazole, pH 8.0. For the PDGF-B/PDGFRβ complex, the reservoir solution is 0.84 M $(NH_4)_2HPO_4$, 0.1 M imidazole, pH 8.0.

X-ray diffraction and data processing. Crystals were cryoprotected in the presence of 30% glycerol in the mother liquor and immediately flash-cooled in liquid nitrogen. X-ray diffraction data were measured at the LS-CAT beamline 21-ID-D, Advanced Photon Source (APS), Argonne, IL. The data were indexed, integrated, and scaled with HKL2000 (3). The PDGF-A/propeptide crystals belonged to the spacegroup $P2_12_12_1$, with cell dimensions $a = 50.84$ Å, $b = 119.21$ Å, and $c = 146.71$ Å. The PDGF-B/PDGFRβ crystals also belonged to the spacegroup $P2_12_12_1$, with cell dimensions $a = 78.47$ Å, $b = 116.82$ Å, and $c = 134.15$ Å.

Structure determination and refinement. To determine the structure of the PDGF-B/PDGFRβ complex, the PDGF-B dimer and the second immunoglobunin domain (D2) of PDGFRβ in the complex were located using the molecular replacement program PHASER (4), with the free PDGF-BB structure (PDB ID: 1PDG) and the D2 domain of VEGFR1 (PDB ID: 1FLT) as the search models. After the PDGF-B dimer and PDGFRβ-D2 were located, PDGFRβ-D1 was manually placed by superposing KIT-D1-D2 (PDB ID: 2O26) onto PDGFRβ-D2. The molecular replacement phases were improved with twofold noncrystallographic symmetry (NCS) averaging, as implemented in the program CNS (5), generating 2*Fo-Fc* electron density maps in which PDGFRβ-D3 was clearly discernible. To determine the structure of the PDGF-A/propeptide complex, the PDGF-A dimer in the complex was located using the molecular replacement program PHASER (4), with the free PDGF-BB structure (PDB ID: 1PDG) as the search model. After obtaining the initial phases, the propeptides were manually traced from NCS-averaged electron density maps. The models were rebuilt using COOT (6), and subjected to simulated annealing, minimization, and group B factor refinements with CNS (5). Water molecules were automatically added with CNS and validated with electron density maps.

Isothermal titration calorimetry. Calorimetric titrations were carried out on a VP-ITC calorimeter (MicroCal) at 30 °C and the data were processed with MicroCal Origin 5.0 software. Before titrations, all proteins used were buffer-exchanged into an identical lot of HBS buffer (10 mM Hepes pH7.5, 150 mM NaCl) using gel filtration to control buffer heat dilution effects. The protein samples were thoroughly degassed before the experiments. Because PDGFRs can be expressed at higher levels than the ligands, the receptor proteins were chosen as the titrants, and the ligands were placed in the reaction chamber during the experiments.

1. Reeves PJ, Callewaert N, Contreras R, Khorana HG (2002) Structure and function in rhodopsin: high-level expression of rhodopsin with restricted and homogeneous N-glycosylation by a tetracycline-inducible N-acetylglucosaminyltransferase I-negative HEK293S stable mammalian cell line. *Proc Natl Acad Sci USA* 99:13419–13424.
2. Dukkipati A, Park HH, Waghray D, Fischer S, Garcia KC (2008) BacMam system for high-level expression of recombinant soluble and membrane glycoproteins for structural studies. *Protein Expr Purif* 62:160–170.
3. Otwinowski Z, Minor W (1997) Processing of X-ray diffraction data collected in oscillation mode. *Methods Enzymol* 276:307–326.
4. McCoy AJ, et al. (2007) Phaser crystallographic software. *J Appl Cryst* 40:658–674.
5. Brunger AT, et al. (1998) Crystallography & NMR system: A new software suite for macromolecular structure determination. *Acta Crystallogr D* 54:905–921.
6. Emsley P, Cowtan K (2004) COOT: model-building tools for molecular graphics. *Acta Crystallogr D* 60:2126–2132.

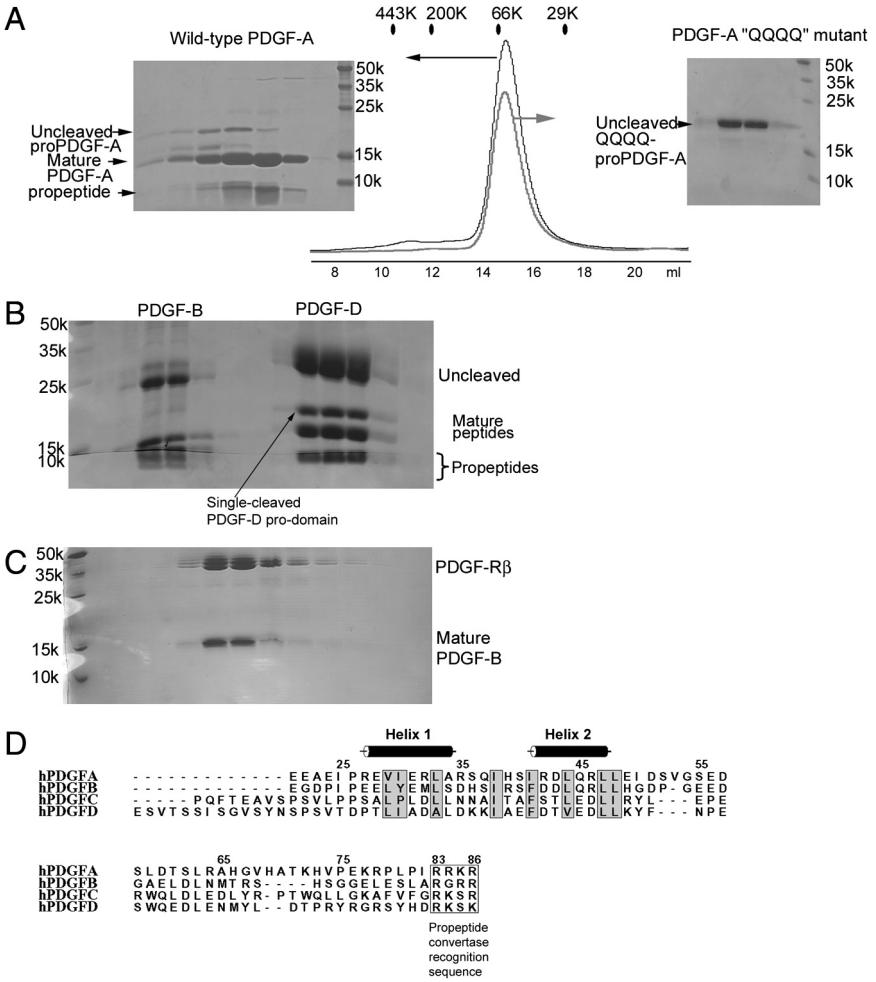

Fig. S1. Recombinant PDGFs contain noncovalently associated propeptides. (*A*) Gel filtration analysis of the complex between the propeptide and mature PDGF-A, comparing wild type and a cleave site mutant with unprocessed pro-PDGF-A. (*B*) SDS-PAGE of the recombinant PDGF-B and PDGF-D proteins captured by C-terminal his-tag, showing that PDGF-B and PDGF-D also have noncovalently associated propeptides of similar length. (*C*) The mature PDGF-B:PDGFRβ complex purified from expression constructs containing the PDGF-B prosequence, showing that the receptor can displace the prosequence from mature PDGF-B. This complex was subsequently used for crystallization and structure determination. (*D*) Sequence alignment of the regions preceding the growth factor domains of PDGFs, showing that the hydrophobic residues important for binding the growth factor domain are conserved in the PDGF prosequences.

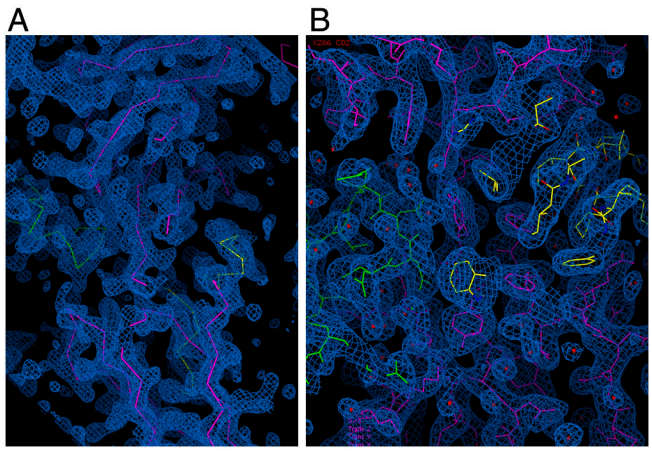

Fig. S2. The NCS-averaged, SIGMAA-weighted 2*Fo-Fc* electron density maps of the PDGF-B:PDGFRβ-D1-D3 complex. (*A*) The fitting of the Cα traces of the final model to the electron density map. (*B*) A close-up view of the PDGF-B:PDGFRβ-D1-D3 interface, focusing on the cluster of hydrophobic residues from both the ligand and the receptor. The carbon atoms for the protein models are colored pink for the receptor, yellow and green for PDGF-B.

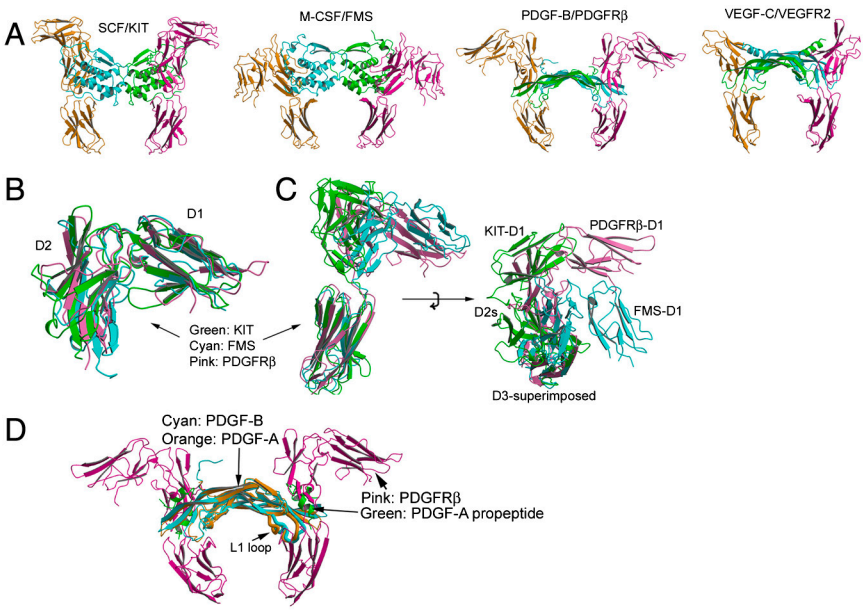

Fig. S3. Comparison of the PDGF-B:PDGFRβ complex with related structures. (*A*) Side-by-side comparison of the PDGF-B:PDGFRβ-D1-D3 complex, the SCF/KIT-D1-D3 complex, the M-CSF/FMS-D1-D3 complex, and the VEGF-C/VEGFR2-D2-D3 complex, showing that the D3 positions in these complexes are roughly similar. (*B*) The D1–D2 modules of KIT and FMS can be superposed to that of PDGFRβ, with an rms deviation of 2.2 Å between KIT and PDGFRβ for 104 matching Cα atoms, and an rms deviation of 1.9 Å between FMS and PDGFRβ for 97 matching Cα atoms. (*C*) The difference between KIT, FMS, and PDGFRβ lies primarily in the orientation of D2, which leads to dramatically different positions of D1, as revealed by the overlaying of their D3 domains. The rms deviation is 2.4 Å between KIT-D3 and PDGFRβ-D3 for 47 matching Cα atoms, and is 2.3 Å between FMS-D3 and PDGFRβ-D3 for 54 matching Cα atoms. (*D*) Superposition of the PDGF-B:PDGFRβ complex with the PDGF-A/propeptide complex by overlaying the PDGFs, showing that PDGFRβ and the propeptide occupy overlapping sites on PDGFs. The superposition of the two complexes also shows that the PDGF-A and PDGF-B L1 loops have similar conformations. The rms deviation is 1.2 Å between PDGF-A and PDGF-B for 172 matching Cα atoms.

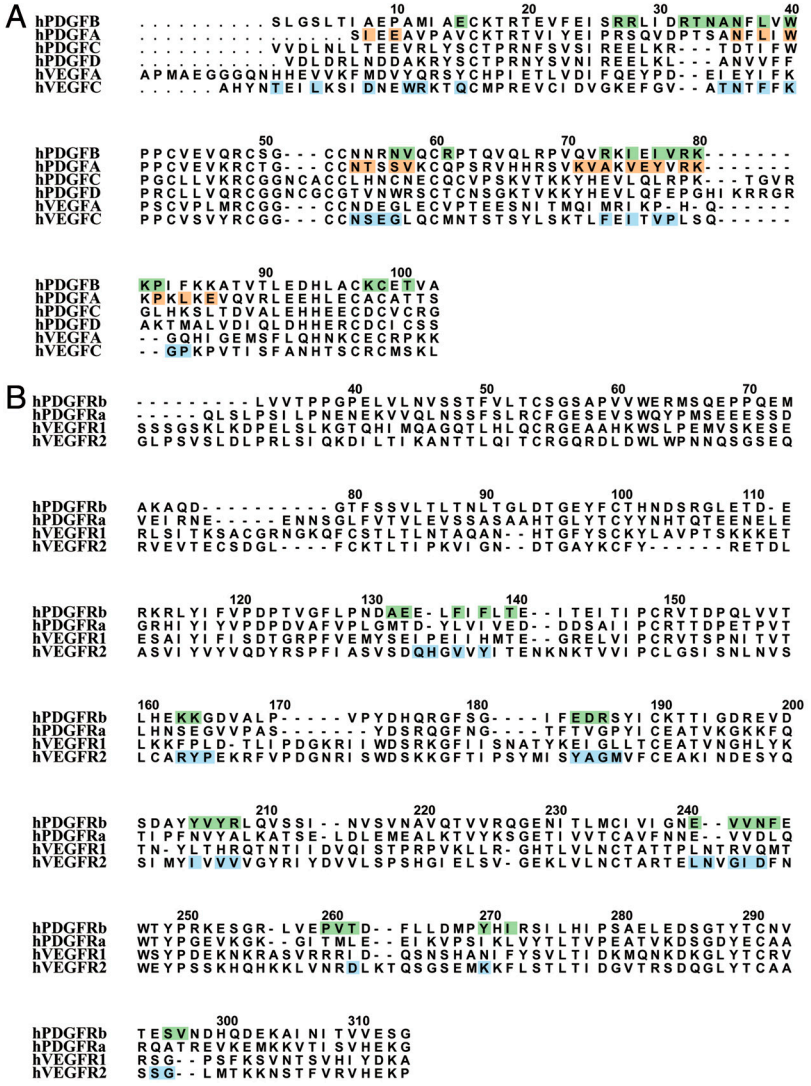

Fig. S4. Sequence alignment of PDGFs and PDGFRs, with VEGFs and VEGFRs included for comparison. The interface-contributing residues in the PDGF-B:PDGFRβ complex are shaded in green. The interface-contributing residues in the VEGF-C:VEGFR2 complex are shaded in cyan. The PDGF-A residues involved in propeptide-binding are shaded in orange.

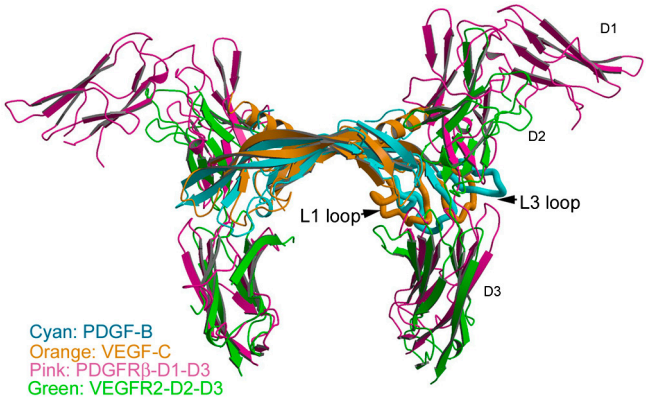

Fig. S5. Comparison of the PDGF-B:PDGFRβ-D1-D3 complex and the VEGF-C:VEGFR2-D2-D3 complex by superposition of the ligands PDGF-B and VEGF-C, showing that the receptor D2 and D3 domains have roughly similar orientations, and the D2 domains are the most different, due to the structural differences between PDGF-B and VEGF-C. The rms deviation is 1.7 Å between VEGF-C and PDGF-B for 132 matching Cα atoms. The L1 and L3 loops of PDGF-B and VEGF-C are highlighted as thicker tubes.

Table S1. Data collection and refinement statistics

	PDGF-B/PDGFRβ complex	PDGF-A/propeptide complex
Data collection		
Spacegroup	$P2_12_12_1$	$P2_12_12_1$
Unit cell (*a*, *b*, *c*) (Å)	78.47, 116.82, 134.15	50.84, 119.21, 146.71
Wavelength (Å)	0.9786	0.9786
Resolution range (Å) (highest resolution shell)	20–2.3 (2.4–2.3)	30–2.4 (2.55–2.4)
Unique reflections	54,767	45,306
Completeness (%)	98.8 (97.7)	98.1 (97.9)
I/σ (I)	14.3 (3.3)	15.6 (3.5)
Redundancy	4.0	5.7
R_{merge} (%)*	7.8 (32.7)	6.8 (37.7)
R_{meas} (%)*	6.2 (42.6)	7.4 (44.6)
Refinement		
Resolution range (Å) (highest resolution shell)	20–2.3 (2.4–2.3)	20–2.4 (2.55–2.4)
R_{cryst}†	0.238 (0.342)	0.225 (0.385)
R_{free}†	0.278 (0.359)	0.276 (0.389)
Average B factor (Å^2) (protein, solvent)	66.3, 69.3	65.4, 68.7
rmsd bond length (Å)	0.009	0.009
rmsd bond angle (°)	1.6	1.5
Ramachandran (favored, allowed, generally allowed, disallowed) (%)	85.2, 13.4, 1.4, 0	85.9, 12.9, 1.2, 0

*$R_{merge} = \sum_{hkl}|I\text{-}\langle I\rangle|/\sum_{hkl}I$, where I is the intensity of unique reflection hkl, and $\langle I\rangle$ is the average over symmetry-related observation of unique reflection hkl. R_{meas} is redundancy-independent R factor.

†$R_{cryst} = \sum|F_{obs}\text{-}F_{calc}|/\sum F_{obs}$, where F_{obs} and F_{calc} are the observed and the calculated structure factors, respectively. R_{free} is calculated using 5% of reflections sequestered before refinement.

Table S2. Contacts between the propeptide and PDGF-A

The propeptide		The protruding PDGF-A protomer	The receding PDGF-A protomer		Distance (Å)
		Salt bridges			
Glu22		Arg159			3.1
		Hydrogen bonds			
Leu33	O		Asn134	ND2	2.9
Ser36	O		Asn134	ND2	2.8
Ile41	N		Glu90	OE1	3.2
		Van der Waals contacts			
Glu22		Arg159			
Ala23		Tyr157, Arg159			
Glu24		Asn116, Tyr157			
Ile25		Asn116, Glu156, Tyr157			
Pro26		Tyr157, Lys160			
Val29		Tyr157			
Ile30		Leu118			
Ile30				Thr135, Ser137	
Arg32		Tyr157			
Leu33		Leu118		Asn134, Thr135	
Ala34				Asn134, Val138	
Ser36				Asn134	
Gln37				Asn134	
Ile38		Trp120			
His39		Trp120			
Ser40		Trp120		Glu90	
Ile41		Trp120, Lys151,Val152, Ala153, Val155, Leu164, Glu166		Glu90	
Leu44		Trp120, Ala153, Leu164, Glu166			
Leu48		Tyr157, Pro162			
Glu49		Pro162			
Ile50		Pro162			
Leu53		Leu164			
Arg83		Glu166			
Arg84				Ile88	
Lys85				Ile88	
Arg86				Ile88	

Table S3. Contacts between PDGF-B and PDGFRβ

PDGFRβ		The protruding PDGF-B protomer		The receding PDGF-B protomer		Distance (Å)
			Salt bridges			
Glu133		Lys81				3.4
Lys163				Glu15		3.3
			Hydrogen bonds			
Asp185	OD2			Asn55	ND2	2.5
Arg186	NE			Cys99	O	3.0
Arg186	NH2			Cys99	O	3.1
Arg186	O			Asn54	ND2	3.1
Val206	O			Asn54	ND2	2.9
Tyr207	OH			Asn55	OD1	3.2
Glu241	O	Arg27	NH1			2.8
Glu241	O	Arg27	NH2			2.5
Val243	N	Ala35	O			2.7
Val243	O	Asn36	N			3.1
Asn244	OD1	Asn34	ND2			2.8
Phe245	N	Asn34	OD1			3.1
Thr262	N	Arg32	O			2.7
Thr262	O	Arg28	NH1			3.0
Ser296	O	Arg79	N			2.9
			Van der Waals contacts			
Ala132				Arg73, Phe84,		
Glu133				Pro82, Lys81, Phe84		
Phe136				Phe84, Arg73, Trp40		
Phe138				Ile77, Leu38, Pro82, Lys80		
Thr140				Lys80		
Lys163		Glu15				
Lys164		Glu15				
Glu184		Thr101				
Asp185		Asn54, Asn55, Asn57, Val58				
Arg186		Asn54, Lys98, Cys99				
Tyr205		Asn54		Trp40		
Val206		Asn54				
Tyr207		Asn54, Asn55		Leu38		
Arg208		Asn55, Asn57				
Glu241		Asn55		Arg27, Leu38		
Val242				Arg27, Ala35, Asn36, Phe37		
Val243				Ala35, Asn36, Asn34		
Asn244				Asn34, Asn36		
Phe245				Asn34		
Pro260				Thr33, Arg32		
Val261				Arg32, Arg28		
Thr262				Arg32, Thr33, Asn34, Arg28		
Phe264				Arg27		
Tyr270		Arg56				
Ile272				Ala35		
Ser296				Val78		
Val297				Ile77		